Available online at www.sciencedirect.com
ScienceDirect
Journal of Sound and Vibration 300 (2007) 280–291
JOURNAL OF SOUND AND VIBRATION
www.elsevier.com/locate/jsvi

Natural frequencies and mode shapes of arbitrary beam structures with arbitrary boundary conditions

S.M. Wiedemann

Lenaustrasse 2, 81373 Munich, Germany

Received 17 November 2005; received in revised form 7 July 2006; accepted 9 August 2006
Available online 10 October 2006

Abstract

Generalising the method presented in an earlier paper an analytical solution is presented for the natural frequencies, mode shapes and orthogonality conditions of an arbitrary system of Euler–Bernoulli beams interconnected by arbitrary joints and subject to arbitrary boundary conditions.

1. Introduction

In an earlier paper [1] the author and a colleague presented an analytical method to get exact solutions for the natural frequencies and mode shapes of a free–free beam with large end masses. The beams were analysed within the boundaries of linear theory of elasticity (Euler–Bernoulli beams). Here, the method outlined in Ref. [1] is extended to apply also to a series of beams interconnected by arbitrary joints and subject to arbitrary boundary conditions. Thus the present paper presents the general principle underlying the results presented for special setups of beams (for example in Refs. [1,2]) and may give a general answer to any similar problems.

2. Determination of boundary conditions

The equation of motion of a beam with mass per unit length m_b and flexural stiffness EI, neglecting rotary inertia and shear force, is given as (see for example Ref. [3])

$$EI\, y^{\mathrm{iv}}(x,t) + m_b \ddot{y}(x,t) = 0, \tag{1}$$

It is well known that using the method of separation of variables the solution to Eq. (1) yields the eigenfunctions for the ith mode shape as

$$y_i(x) = A\, \sin(kx) + B\, \cos(kx) + C\, \sinh(kx) + D\, \cosh(kx), \tag{2}$$

where

$$k^2 = \omega_i \sqrt{\frac{m_b}{EI}} \tag{3}$$

E-mail address: Simon.wiedemann@web.de.

0022-460X/$ - see front matter
doi:10.1016/j.jsv.2006.08.012

and ω_i is the ith natural frequency. The arbitrary constants are eliminated from Eq. (2) by means of the four boundary conditions at $x = 0$ and L.

Although the readers are probably familiar with the above equations and their implications, no paper to the author's knowledge has so far attempted to outline a general approach to a series of beams connected with arbitrary joints and subject to arbitrary boundary conditions.

The key to the analytical solution aimed at in this paper is the use of the tangent frame for the description of the beam boundary conditions. Thus it is mandatory to describe the boundary conditions of each beam *relative* to the previous beam within the chain. For each beam, *all following masses*, including any following beams, *must be projected onto that* point upon the *beam* where the following mentioned masses are attached to. Let us illustrate this using various examples.

We reconsider first the example given in Ref. [1] and shown in Fig. 1, with end masses M_i and rotary inertias I_{0i} about the ends of the beam. G_i are the centres of masses, λ_i the torsional springs stiffnesses, and EI, m_b and L the usual notation for the uniform beam.

Let us now project all masses onto those points of the beam where they are attached to. Since the situation at both ends of the beam is analogous, we only consider the boundary condition at $x = 0$. To this end we introduce angle α_1 to be the rotation of M_1 relative to the beam due to the torsional spring stiffness λ_1.

Thus in reality during vibration M_1 would rotate through angles $\pm\alpha_1$ about the angle of equilibrium θ_1, but to be able to set up the equations for the boundary conditions it must be assumed that angle α_1 remains small and thus does not significantly change θ_1 during vibration. This assumption seems just, considering the fact that for the beams too, only linear theory of elasticity for small deflections is applied.

Fig. 2 shows the boundary condition geometry at $x = 0$, where $y(0)$ is the deflection and $y'(0)$ the slope of the beam, and θ_1 the fixed angle between O_1G_1 and the undeformed beam axis. Angle α_1 is the rotation of the mass relative to the beam due to the torsion spring of stiffness λ_1.

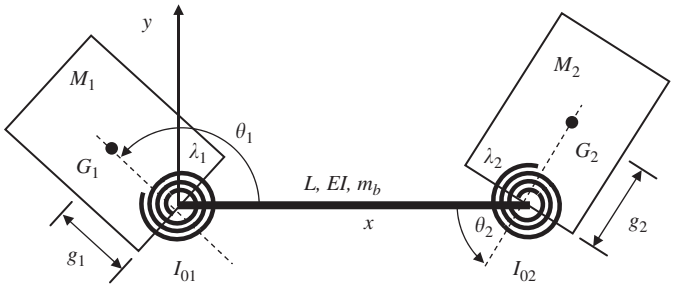

Fig. 1. Free–free beam with end masses and torsion springs ([1], no gravity!).

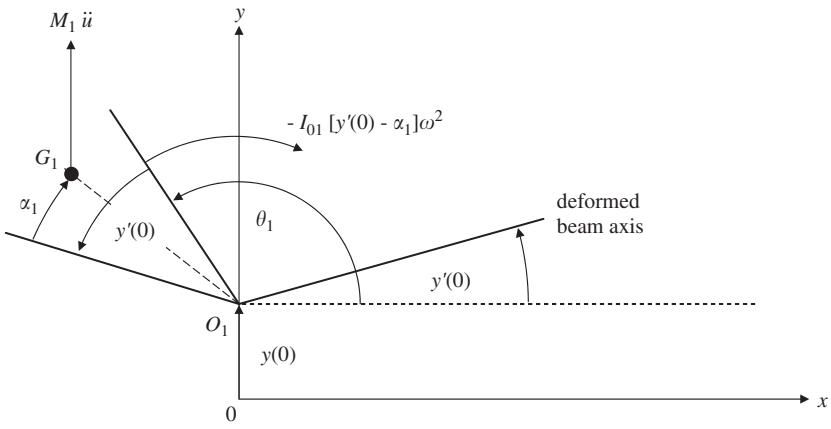

Fig. 2. Boundary conditions at $x = 0$ [1].

First we note that,

$$\alpha_1 = \frac{EI\, y''(0)}{\lambda_1}. \tag{4}$$

Bending moment equilibrium: G_1 is accelerated by $\ddot{u} = -y(0)\omega^2$ perpendicular to the beam. From this, the moment about O_1 is $-M_1 g_1 \omega^2 y(0) \cos\theta_1$. Similarly the rotary inertia of the mass produces a moment about O_1 which is equal to $-I_{01}\omega^2[y'(0) - \alpha_1]$. Hence we have

$$EI\, y''(0) = -I_{01}\omega^2[y'(0) - \alpha_1] - g_1 M_1 \omega^2[y(0)\cos\theta_1]. \tag{5}$$

Shear force equilibrium: The total acceleration of G_1 is due to the transverse acceleration $\omega^2 y(0)$ and the rotational acceleration $g_1[y'(0) - \alpha_1]\omega^2$. Hence resolving the second term perpendicular to the beam, the total shear force is

$$EI\, y'''(0) = M_1\omega^2 y(0) + g_1 M_1 \omega^2[y'(0) - \alpha_1]\cos\theta_1. \tag{6}$$

It was mentioned before that the boundary conditions at $x = L$ are similar. Substituting the four boundary condition equations gained this way into Eq. (2) and collecting the various terms with respect to A, B, C and D we can set up a system of equations as

$$\begin{bmatrix} d_{11} & d_{12} & d_{13} & d_{14} \\ d_{21} & d_{22} & d_{23} & d_{24} \\ d_{31} & d_{32} & d_{33} & d_{34} \\ d_{41} & d_{42} & d_{43} & d_{44} \end{bmatrix} \begin{bmatrix} A \\ B \\ C \\ D \end{bmatrix} = \mathbf{0} \tag{9}$$

and since A, B, C and D are non-zero in general, a non-trivial solution must satisfy

$$\det[d_{nm}] = \mathbf{0}. \tag{10}$$

Using the notation $C = \cos(kL)$, $S = \sin(kL)$, $Ch = \cosh(kL)$ and $Sh = \sinh(kL)$ results in the following expressions for the d_{nm}:

$$\begin{aligned}
d_{11} &= d_{13} = I_{01} k\omega^2, \\
d_{12} &= -EI\, k^2 + \frac{EI\, I_1 k^2 \omega^2}{\lambda_1} + g_1 M_1 \omega^2 \left[\frac{EI\, g_1 k^2}{\lambda_1} + \cos\theta_1\right], \\
d_{14} &= EI\, k^2 - \frac{EI\, I_1 k^2 \omega^2}{\lambda_1} + g_1 M_1 \omega^2 \left[-\frac{EI\, g_1 k^2}{\lambda_1} + \cos\theta_1\right], \\
d_{21} &= EI\, k^3 + g_1 k M_1 \omega^2 \cos\theta_1, \\
d_{22} &= M_1 \omega^2 \left[1 + \frac{EI\, g_1 k^2 \cos\theta_1}{\lambda_1}\right], \\
d_{23} &= -EI\, k^3 + g_1 k M_1 \omega^2 \cos\theta_1, \\
d_{24} &= M_1 \omega^2 \left[1 - \frac{EI\, g_1 k^2 \cos\theta_1}{\lambda_1}\right], \\
d_{31} &= EI\, k^2 S + g_2 M_2 \omega^2 \cos\theta_2 S + I_{02}\left[kC - \frac{EI\, k^2 S}{\lambda_2}\right]\omega^2, \\
d_{32} &= EI\, k^2 C + g_2 M_2 \omega^2 \cos\theta_2 C - I_{02}\left[kS + \frac{EI\, k^2 C}{\lambda_2}\right]\omega^2,
\end{aligned}$$

$$d_{33} = g_2 M_2 \omega^2 \cos\theta_2 Sh - EI\,k^2 Sh + I_{02}\left[kCh + \frac{EI\,k^2 Sh}{\lambda_2}\right]\omega^2,$$

$$d_{34} = g_2 M_2 \omega^2 \cos\theta_2 Ch - EI\,k^2 Ch + I_{02}\left[kSh + \frac{EI\,k^2 Ch}{\lambda_2}\right]\omega^2,$$

$$d_{41} = -EI\,k^3 C + M_2\omega^2 S + M_2\omega^2 g_2 \cos\theta_2\left[kC - \frac{EI\,k^2 S}{\lambda_2}\right],$$

$$d_{42} = EI\,k^3 S + M_2\omega^2 C - M_2\omega^2 g_2 \cos\theta_2\left[kS + \frac{EI\,k^2 C}{\lambda_2}\right],$$

$$d_{43} = EI\,k^3 Ch + M_2\omega^2 Sh + M_2\omega^2 g_2 \cos\theta_2\left[kCh + \frac{EI\,k^2 Sh}{\lambda_2}\right],$$

$$d_{44} = EI\,k^3 Sh + M_2\omega^2 Ch + M_2\omega^2 g_2 \cos\theta_2\left[kSh + \frac{EI\,k^2 Ch}{\lambda_2}\right]. \tag{11}$$

As a second example and based on the analysis of the single flexible beam, let us now consider a double flexible beam system with end mass as shown in Fig. 3, where the dotted lines are the rigid body position of the beams and the solid lines the superimposed elastic deflections. The base is assumed to be inertially fixed, the end mass is rigidly connected to the second beam at O_3, and O_1 and O_2 are pin joints with either rotary inertia or joint stiffness. The cases of rotary inertia or stiffness will be called "unlocked" and "locked", respectively. The second beam is inclined at a fixed angle θ in the undeformed configuration.

Using the notation introduced before in connection with the single flexible beam the deflection shape of each beam l for a natural frequency ω_i $(i = 1 \ldots \infty)$ is given as

$$y_{l,i}(x) = A_{l,i}\sin(k_{l,i}x_l) + B_{l,i}\cos(k_{l,i}x_l) + C_{l,i}\sinh(k_{l,i}x_l) + D_{l,i}\cosh(k_{l,i}x_l), \tag{12}$$

where

$$k_{l,i}^2 = \omega_i\sqrt{\frac{m_{bl}}{EI_l}}, \quad l = 1, 2, \tag{13}$$

where m_{bl} is the mass per unit length of beam l and EI_l the flexural stiffness.

For the boundary conditions of the beams, consider Fig. 3. For a locked Joint2 at O_2 (stiffness) and an unlocked Joint1 at O_1 (rotary inertia I_{g1}), the boundary conditions of Beam1 at $x_1 = 0$ are

$$y_1(0) = 0 \tag{14}$$

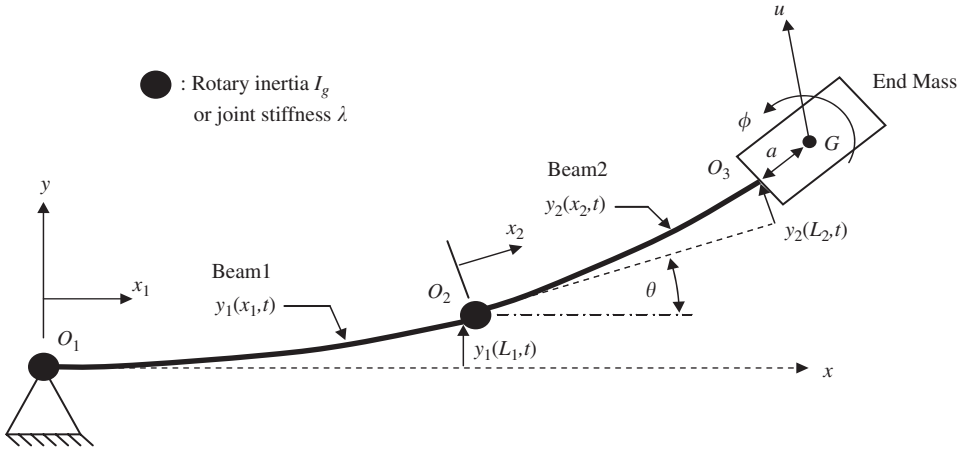

Fig. 3. Double flexible beam system with end mass (no gravity!).

and

$$I_{g1}\omega^2 y_1'(0) = -EI_1\, y_1''(0). \tag{15}$$

Recalling what was said before: *when masses are involved, we must* project all masses onto *those points of* the beams *where they are attached to*. At $x_1 = L_1$, projecting all masses attached to Beam2 (i.e., equilibrium of all forces including translatory forces due to inertia) gives:

$$\begin{aligned} EI_1 y_1''(L_1) = {} & I_p\omega^2\left[y_1'(L_1) + y_2'(L_2)\right] + M_p\omega^2 y_1(L_1)(L_2 + a)\cos\theta \\ & + M_p\omega^2\left[y_2(L_2) + y_2'(L_2)a + y_1'(L_1)(L_2 + a)\right](L_2 + a) \\ & + \int_0^{L_2} m_{b2}\omega^2\left[y_2(x_2) + y_1(L_1)\cos\theta + y_1'(L_1)x_2\right]x_2\,\mathrm{d}x_2 \end{aligned} \tag{16}$$

with M_p and I_p as the mass translatory and rotary inertia, and force equilibrium gives

$$\begin{aligned} EI\, y_1'''(L_1) = {} & -M_p\omega^2\left[y_2(L_2) + y_2'(L_2)a + y_1'(L_1)(L_2 + a)\right]\cos\theta \\ & - \left(M_p + M_2\right)\omega^2 y_1(L_1) - \int_0^{L_2} m_{b2}\omega^2\left(y_2(x_2) + y_1'(L_1)\right)\cos\theta\,\mathrm{d}x_2, \end{aligned} \tag{17}$$

where M_2 is the mass of Beam2. The integrals in Eqs. (16) and (17) are usually negligibly small but must be included for very small or zero end masses to get better results for the natural frequencies.

Note that it was stressed in the beginning that the tangent frame formulation is used, and thus the boundary conditions for Beam2 at $x_2 = 0$ are (relative to Beam1!):

$$y_2(0) = 0 \tag{18}$$

and

$$\lambda_2 y_2'(0) = EI_2\, y_2''(0). \tag{19}$$

The projection of all masses attached to the end of Beam2 at $x_2 = L_2$ (i.e., equilibrium of all rotary forces including rotary forces due to inertia) gives:

$$\begin{aligned} EI_2 y_2''(L_2) = {} & I_p\omega^2\left(y_1'(L_1) + y_2'(L_2)\right) \\ & + M_p\omega^2\left[y_2(L_2) + y_2'(L_2)a + y_1'(L_1)(L_2 + a) + y_1(L_1)\cos\theta\right]a \end{aligned} \tag{20}$$

and force equilibrium gives

$$EI\, y_2'''(L_2) = -M_p\omega^2\left[y_2(L_2) + y_2'(L_2)a + y_1'(L_1)(L_2 + a) + y_1(L_1)\cos\theta\right]. \tag{21}$$

Applying the boundary conditions and collecting all terms with respect to $A_{1,i}$, $B_{1,i}$, $C_{1,i}$, $D_{1,i}$, $A_{2,i}$, $B_{2,i}$, $C_{2,i}$ and $D_{2,i}$, gives a matrix similar to that in Eq. (9) but with 8×8 elements due to the eight boundary condition equations. However, with Eqs. (14) and (18), implying that $D_{1,i} = -B_{1,i}$ and that $D_{2,i} = -B_{2,i}$, here the matrix reduces to:

$$\begin{bmatrix} d_{11} & d_{12} & d_{13} & d_{14} & d_{15} & d_{16} \\ d_{21} & d_{22} & d_{23} & d_{24} & d_{25} & d_{26} \\ d_{31} & d_{32} & d_{33} & d_{34} & d_{35} & d_{36} \\ d_{41} & d_{42} & d_{43} & d_{44} & d_{45} & d_{46} \\ d_{51} & d_{52} & d_{53} & d_{54} & d_{55} & d_{56} \\ d_{61} & d_{62} & d_{63} & d_{64} & d_{65} & d_{66} \end{bmatrix} \begin{bmatrix} A_{1,i} \\ B_{1,i} \\ C_{1,i} \\ A_{2,i} \\ B_{2,i} \\ C_{2,i} \end{bmatrix} = \mathbf{0} \tag{22}$$

and as before, a non-trivial solution must satisfy

$$\det[d_{nm}] = \mathbf{0}. \tag{23}$$

Neglecting the integral terms in Eqs. (16) and (17) and using the notation $C_1 = \cos(k_1 L_1)$, $S_1 = \sin(k_1 L_1)$, $Ch_1 = \cosh(k_1 L_1)$, $Sh_1 = \sinh(k_1 L_1)$, $C_2 = \cos(k_2 L_2)$, $S_2 = \sin(k_2 L_2)$, $Ch_2 = \cosh(k_2 L_2)$, $Sh_2 = \sinh(k_2 L_2)$,

the elements d_{nm} in Eqs. (22) and (23) are given as

$$
\begin{aligned}
&d_{11} = d_{13} = I_{g1}k_1\omega^2, \quad d_{12} = -2EI_1k_1^2, \quad d_{14} = d_{15} = d_{16} = 0,\\
&d_{21} = k_1\big(I_p + M_p(L_2+a)^2\big)\omega^2C_1 + S_1\big(EI_1k_1^2 + M_p(L_2+a)\omega^2\cos\theta\big),\\
&d_{22} = C_1\big(EI_1k_1^2 + M_p(L_2+a)\omega^2\cos\theta\big) + Ch_1\big(EI_1k_1^2 - M_p(L_2+a)\omega^2\cos\theta\big)\\
&\qquad - k_1\big(I_p + M_p(L_2+a)^2\big)\omega^2(S_1+Sh_1),\\
&d_{23} = k_1\big(I_p + M_p(L_2+a)^2\big)\omega^2Ch_1 + \big(-EI_1k_1^2 + M_p(L_2+a)\omega^2\cos\theta\big)Sh_1,\\
&d_{24} = \omega^2(L_2+a)M_pS_2 + \omega^2k_2\big(I_p + M_p(L_2+a)a\big)C_2,\\
&d_{25} = \omega^2(L_2+a)M_p(C_2-Ch_2) - \omega^2k_2\big(I_p + a(L_2+a)M_p\big)(S_2+Sh_2),\\
&d_{26} = \omega^2k_2\big(I_p + M_p(L_2+a)a\big)Ch_2 + \omega^2(L_2+a)M_pSh_2,\\
&d_{31} = \big(M_2+M_p\big)\omega^2S_1 + k_1C_1\big(-EI_1k_1^2 + M_p(L_2+a)\omega^2\cos\theta\big),\\
&d_{32} = \big(M_2+M_p\big)\omega^2(C_1-Ch_1) + EI_1k_1^3(S_1-Sh_1)\\
&\qquad - k_1(L_2+a)M_p\omega^2\cos\theta(S_1+Sh_1),\\
&d_{33} = \big(M_2+M_p\big)\omega^2Sh_1 + k_1Ch_1\big(EI_1k_1^2 + M_p(L_2+a)\omega^2\cos\theta\big),\\
&d_{34} = \omega^2\cos\theta M_p(S_2 + ak_2C_2),\\
&d_{35} = \omega^2\cos\theta M_p(C_2 - Ch_2 + ak_2(S_2+Sh_2)),\\
&d_{36} = \omega^2\cos\theta M_p(Sh_2+Ch_2), \quad d_{41} = d_{42} = d_{43} = 0,\\
&d_{44} = d_{46} = k_2\lambda_2, \quad d_{45} = 2EI_2k_2^2,\\
&d_{51} = \omega^2\cos\theta M_paS_1 + \omega^2k_1\big(I_p + M_p(L_2+a)a\big)C_1,\\
&d_{52} = \omega^2\cos\theta M_pa(C_1-Ch_1) - \omega^2k_1\big(I_p + M_p(L_2+a)a\big)(S_1+Sh_1),\\
&d_{53} = \omega^2k_1\big(I_p + M_p(L_2+a)a\big)Ch_1 + \omega^2\cos\theta M_paSh_1,\\
&d_{54} = k_2\big(I_p + a^2M_p\big)\omega^2C_2 + \big(EI_2k_2^2 + aM_p\omega^2\big)S_2,\\
&d_{55} = \big(EI_2k_2^2 + aM_p\omega^2\big)C_2 + \big(EI_2k_2^2 - aM_p\omega^2\big)Ch_2\\
&\qquad - k_2\big(I_p + a^2M_p\big)\omega^2(S_2+Sh_2),\\
&d_{56} = k_2\big(I_p + a^2M_p\big)\omega^2Ch_2 + \big(-EI_2k_2^2 + aM_p\omega^2\big)Sh_2,\\
&d_{61} = M_p\omega^2(k_1(L_2+a)C_1 + \cos\theta S_1),\\
&d_{62} = M_p\omega^2(-k_1(L_2+a)(S_1+Sh_1) + \cos\theta(C_1-Ch_1)),\\
&d_{63} = M_p\omega^2(k_1(L_2+a)Ch_1 + \cos\theta Sh_1),\\
&d_{64} = -EI_2k_2^3C_2 + M_p\omega^2(ak_2C_2 + S_2),\\
&d_{65} = -M_p\omega^2(-C_2 + Ch_2 + ak_2(S_2+Sh_2)) + EI_2k_2^3(S_2-Sh_2),\\
&d_{66} = EI_2k_2^3Ch_2 + M_p\omega^2(ak_2Ch_2 + Sh_2).
\end{aligned}
\tag{24}
$$

For a locked Joint1, Eq. (15) becomes $\lambda y_1'(0) = EI_1y_1''(0)$, and the elements d_{11} and d_{13} in Eq. (24) are then given by

$$d_{11} = d_{13} = -k_1\lambda_1, \tag{25}$$

where λ_1 denotes the joint stiffness of Joint1.

For an unlocked Joint2, Eq. (19) becomes $I_{g2}\omega^2y_2'(0) = -EI_2y_2''(0)$, and in that case the elements d_{44} and d_{46} in Eq. (24) are:

$$d_{44} = d_{46} = -I_{g2}k_2\omega^2, \tag{26}$$

where I_{g2} is the rotary inertia connected to Beam2 at Joint2.

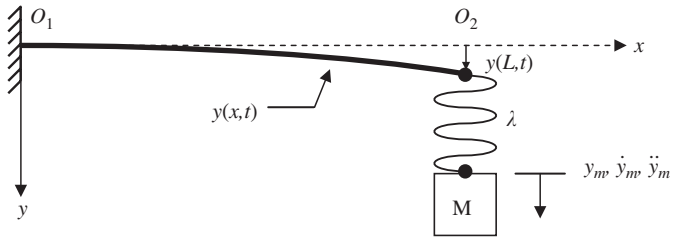

Fig. 4. Single flexible beam with spring and end mass in series (no gravity!).

As so far only rotary stiffness has been taken into account at the various joints in the above example beam structures, consider Fig. 4, where a translational spring stiffness is incorporated.

We apply the principle of mass projection mentioned repeatedly before and find that at joint O_1 ($x = 0$), no masses are attached. The kinematic boundary conditions yield:

$$y(0) = 0 \tag{27}$$

and

$$y'(0) = 0. \tag{28}$$

At joint O_2 ($x = L$), mass M is attached to the beam end via a spring with stiffness λ. However, there is no rotary (inertia) force acting upon the beam end, thus with EI being the beam flexural stiffness,

$$EI\, y''(L) = 0. \tag{29}$$

Incorporating the mass and spring for the second boundary equation at $x = L$, translatory force equilibrium demands that:

$$EI\, y'''(L) = (y_m - y(L))\lambda, \tag{30}$$

where from Fig. 4, y_m denotes the position of the mass along y, relative to some static equilibrium position y_{m0}. It is also clear however that:

$$(y_m - y(L))\lambda = \ddot{y}_m M \tag{31}$$

and that

$$\ddot{y}_m M = -\omega^2 y_m M. \tag{32}$$

On inserting Eq. (32) into Eq. (31), we get

$$(y_m - y(L))\lambda = -\omega^2 y_m M \tag{33}$$

which can be solved for y_m to finally give

$$y_m = \frac{y(L)\lambda}{\lambda + \omega^2 M}. \tag{34}$$

Replacing the right-hand side of Eq. (30) with the right-hand side of Eq. (32) and substituting the y_m with Eq. (34) gives:

$$EIy'''(L) = -\omega^2 \left(\frac{y(L)\lambda}{\lambda + \omega^2 M}\right) M = -\frac{y(L)\lambda\omega^2 M}{\lambda + \omega^2 M}. \tag{35}$$

Finally representing the boundary condition for a spring and mass in series.

With some basic considerations we can make a simple check whether the above equation could be correct at all. First assume that $M = 0$, which must of course result in the shear force being equal to zero and therefore independent of the value of λ. In fact, inserting $M = 0$ in Eq. (35), the right-hand side does become zero, thus giving the expected result. The same is true when inserting $\lambda = 0$, implying that the mass is not at all connected to the beam end. Note here that we cannot at the same time set $M = 0$ and $\lambda = 0$, for in this case the

denominator in Eq. (35) is not defined. For $\lambda \to \infty$, we expect that the mass is practically directly connected to the beam end and indeed, letting $\lambda \to \infty$ in Eq. (35) yields $EI\,y'''(L) = -y(L)\omega^2 M$. The section on numerical results give further supporting evidence for the correctness of Eq. (35).

With Eqs. (27) and (28) we find that in the present case, Eq. (2) implies that:

$$C = -A \tag{36}$$

and that

$$D = -B, \tag{37}$$

so that for the case at hand, Eq. (9) for the characteristic determinant simplifies to give:

$$\begin{bmatrix} d_{11} & d_{12} \\ d_{21} & d_{22} \end{bmatrix} \begin{bmatrix} A \\ B \end{bmatrix} = \mathbf{0}. \tag{38}$$

With the known notation, collecting the terms with respect to A and B gives:

$$\begin{aligned} d_{11} &= \frac{\omega^2 M\lambda(S - Sh)}{\omega^2 M + \lambda} - EI\,k^3(C + Ch), \\ d_{12} &= \frac{\omega^2 M\lambda(C - Ch)}{\omega^2 M + \lambda} + EI\,k^3(S - Sh), \\ d_{21} &= -EI\,k^2(S + Sh), \\ d_{22} &= -EI\,k^2(C + Ch). \end{aligned} \tag{39}$$

From the foregoing examples it is assumed that the reader is now familiar with the proposed principle of determining the boundary conditions for a set of Euler–Bernoulli beams interconnected by arbitrary joints and/or springs and subject to arbitrary dynamical and kinematic boundary conditions. The combination of the examples presented here should enable the reader to find the boundary conditions for any similar problem, but it is pointed out that writing the equations down by hand and collecting the terms as shown above to arrive at the characteristic determinant can become very tedious and prone to errors. It is therefore recommended to use algebraic manipulators which are able to handle symbolic calculations such as MATHEMATICA or Maple.

The question may strike the reader as to why we do not set up the boundary conditions taking into account any possible situation, e.g. translatory and rotatory masses and springs, and thus obtain a general theory. This was the approach followed in the second example with the double flexible beam system, where we distinguished between the cases of locked and unlocked joints and also gave different elements of the characteristic determinant for the two cases at each joint (Eqs. (25) and (26)). However, it is one of the findings of experimenting with the proposed principle for formulating the boundary equations that the simpler these are, the more exact the results will be. Thus we always aimed at taking only the necessary boundary conditions into account and not incorporating some that are irrelevant to the situation at hand. However, the reader is free to intensively try out various sets of equations.

Regarding this point it is noted that whenever springs are applied we must be careful in view of the actual numerical values we insert. For example, if we want the two end masses in the first example above (see Fig. 1) to be connected to the beam by simple pin joints, we only set the two rotary joint stiffnesses λ_1 and λ_2 to a very small value, say 10^{-5}, but not equal to zero as they appear in some denominators (see Eqs. (4) and (11)). For this reason we distinguished between the locked and unlocked joint case in the more complex second example.

3. Determination of natural frequencies

Having found the correct boundary conditions and having set up the characteristic determinant as described in the previous section, the determinant expression can be solved for the natural frequencies ω_i so that the determinant becomes zero (see Eqs. (10) and (23)).

The actual numerical calculation of the ω_i is typically the domain of computers with a suitable programme. However, as a workaround the determinant expression, which is a function of ω only, can be analysed even

with a rather simple computer programme for changes in its sign, and a sufficiently narrow approach to the point where the sign changes will indicate a root and thus one natural frequency or eigenfrequency of the system under observation.

Numerous results for the first example, single free–free flexible beam with two end masses, are given in Ref. [1] and shall not be repeated here.

For the second example, two flexible beams with an end mass, numerical results of natural frequencies are presented using the setup of Ref. [4], which is shown in Fig. 5.

To simulate the setup of Ref. [4] the system properties are chosen to be $L_1 = 2\,\mathrm{m}$, $L_2 = 0.4\,\mathrm{m}$, $m_{b1} = 5.4\,\mathrm{kg/m}$, $m_{b2} = 15.0005\,\mathrm{kg/m}$, $EI_1 = 850.5\,\mathrm{N\,m^2}$, $EI_2 = 3000.9\,\mathrm{N\,m^2}$, $M_p = I_p = 0$ and $\theta = 90^\circ$. To create cantilever beams, the spring stiffnesses are set to a very high value, thus $\lambda_1 = \lambda_2 = 10^{10}\,\mathrm{N\,m/rad}$. Note that for correct results as the end mass is zero, the integrals in Eqs. (16) and (17) are taken into account, but were not considered in Eq. (24), which might therefore not be suited for reproducing the results shown in Table 1.

The agreement between the example beam system of Ref. [4] and the results produced here shows that Eqs. (24)–(26) of the previous section are correct for this case.

For the third example from the previous section shown in Fig. 4 we let $L = 3\,\mathrm{m}$, $m_b = 3\,\mathrm{kg/m}$, $EI = 10^5\,\mathrm{N\,m^2}$, $M = 100\,\mathrm{kg}$ and $\lambda = 10^4\,\mathrm{N/m}$. The results are given in Table 2. Note that only for comparison, the table also gives the analytical results from Ref. [3] for a beam with the same properties but without end mass and spring, i.e. a standard clamped-free beam.

It was mentioned before that this section on numerical results will give further supporting evidence for the correctness of the boundary conditions developed for the beam system shown in Fig. 4, especially for Eq. (35).

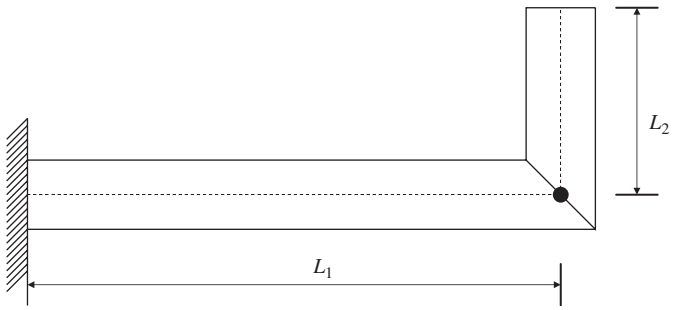

Fig. 5. Example beam system from Ref. [4].

Table 1
First four natural frequencies of example beam system of [4] in comparison with the determinant results

Freq. (rad/s)	[4]	Determinant
ω_1	6.04	6.04
ω_2	44.36	44.36
ω_3	108.13	108.11
ω_4	216.46	216.46

Table 2
First five natural frequencies of the example beam system shown in Fig. 4 with $M = 100\,\mathrm{kg}$ and $\lambda = 10^4\,\mathrm{N/m}$, compared with analytical results of Ref. [3] for the same beam but without end mass and spring (clamped-free)

Freq. (rad/s)	ω_1	ω_2	ω_3	ω_4	ω_5
Determinant	31.02	442.09	1249.82	2451.71	4053.81
Clamped-free	71.33	446.99	1251.59	2452.62	4054.36

Thus by letting $L = 14\,\text{m}$, $m_b = 3.9786\,\text{kg/m}$, $EI = 3 \times 10^6\,\text{N m}^2$, $M = 10^{10}\,\text{kg}$ and $\lambda = 10^{10}\,\text{N/m}$, we effectively produce a pinned end at $x = L$. Table 3 compares the first three eigenfrequencies of a beam with the above properties, computed using Eq. (39), to the analytical results of Ref. [3] for a pinned-clamped beam with the same properties.

4. Determination of mode shapes

The natural frequencies ω_i found by following the procedure described in the previous section can be re-inserted into the boundary condition equation systems (9) or (22), where all the matrix elements are now known. Letting, for example, $A = 1$ in Eq. (9) and deleting any one of the four equations, the remaining three equations can be solved for B–D. Thus knowing A–D and ω_i, these can be inserted into Eq. (2) to yield the ith mode shape $y_i(x)$.

Similarly, letting, for example, $A_{1,i} = 1$ and deleting any one of the six Eq. (22), the other five can be solved to yield $B_{1,i}$, $C_{1,i}$, $A_{2,i}$, $B_{2,i}$ and $C_{2,i}$. Then knowing ω_i and $A_{1,i}$, $B_{1,i}$, $C_{1,i}$, $A_{2,i}$, $B_{2,i}$ and $C_{2,i}$, their insertion into Eq. (12) yields the ith mode shape $y_{l,i}(x)$ for both beams $l = 1, 2$.

For any other beam system the procedure for calculating the mode shapes is similarly followed. It is noted that for further use in dynamic response analyses the mode shapes in their present form may be inconvenient, containing trigonometric and hyperbolic functions and thus causing considerable computational burden. It is therefore possible to use a standard polynomial fit $y(x) = \sum_{n-1}^{N} a_n x^n$ to represent the exact mode shapes. For the first few modes typical orders for N are found to be 7 or 8.

To give a few samples, mode shapes for the third example beam system of sections 2 and 3 are presented in Fig. 6 (mode shapes for the first example beam system in sections 2 and 3 are given in Ref. [1]).

It is seen from Table 2 and Fig. 6 that the example beam system rapidly assumes the properties of a clamped-free beam with the same properties. Experimenting with different values for M and λ provides valuable insight into the behaviour of such beam systems.

5. Orthogonality of mode shapes and numerical accuracy

It is known that any particular solution of the homogeneous partial differential Eq. (1) under some disturbance $F(x,t)$ given as

$$EI\, y^{\text{iv}}(x,t) + m_b \ddot{y}(x,t) = F(x,t), \tag{40}$$

Table 3
First three eigenfrequencies of beam system in Fig. 4 with $M = 10^{10}\,\text{kg}$ and $\lambda = 10^{10}\,\text{N/m}$, compared with analytical results for a clamped-pinned beam [3]

Freq. (rad/s)	[3]	Determinant
ω_1	68.31	68.31
ω_2	221.36	221.36
ω_3	461.86	461.86

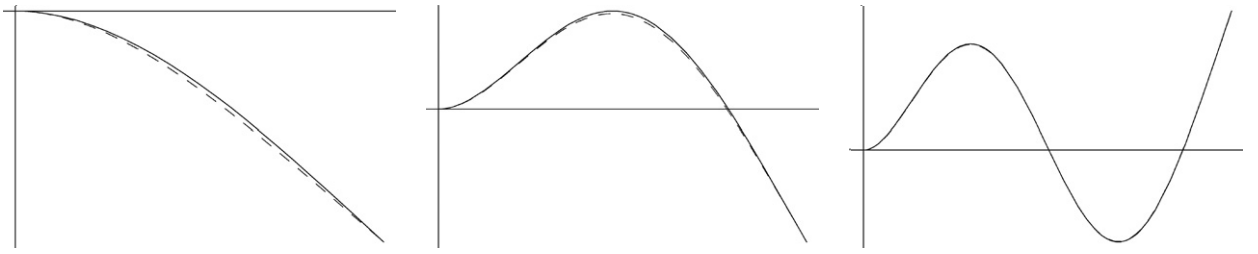

Fig. 6. First three mode shapes of third example beam system (solid) and clamped-free beam (dashed) for the properties given above (see also Table 2).

can be expressed in terms of a superposition of all mode shapes in the form:

$$y(x,t)=\sum_{i=1}^{\infty} y_i(x)q_i(t) \tag{41}$$

which is used for dynamic response analyses.

It is also known that the eigenmodes are orthogonal to each other. But what does this mean? The physical interpretation of the mode shapes of a beam system can be visualised as that of a discrete portion of energy, adding up to the infinite sum of discrete portions of energy expressed in Eq. (41) to finally yield the correct energy related to any true beam motion under arbitrary disturbances.

For us, this means that we have to set up an energy expression in terms of two mode shapes $y_n(x)$ and $y_m(x)$, taking into account the boundary conditions. The final extract of calculations as given for example in [1] is the following rule:

Take the kinetic energy expressed by all boundary conditions, independent of its sign, and add up all terms. When doing this, waive the eigenfrequency ω and replace the beam deflection $y(x)$ with the product of two mode shapes $y_n(x)$ and $y_m(x)$.

We note that kinematic boundary conditions are irrelevant for the energy expressions. Now let us try this for the complex second example of the beam system shown in Fig. 3. The boundary conditions for Beam1 are given by Eqs. (14) through (17), the boundary conditions for Beam2 are given by Eqs. (18) through (21) for the case Joint1 unlocked, Joint2 locked. Now we take all these expressions, add them independent of their signs in the boundary equations, waive the ω and replace the beam deflections by the product of two mode shapes. Note that according to what was said just before, Eqs. (14) and (18) are purely kinematic and thus irrelevant for the case at hand. Letting $y_{n1}(x)$ and $y_{n2}(x)$ be the nth mode shape for Beam1 and Beam2, respectively, the described procedure gives:

$$\begin{aligned}
&\int_0^{L_2} m_{b1}y_{n1}(x_1)y_{m1}(x_1)\,\mathrm{d}x_1+\int_0^{L_2} m_{b2}y_{n2}(x_2)y_{m2}(x_2)\,\mathrm{d}x_2+I_{g1}y'_{n1}(0)y'_{m1}(0)\\
&\quad+I_p\left[y'_{n1}(L_1)y'_{m1}(L_1)\right]\left[y'_{n2}(L_2)y'_{m2}(L_2)\right]+M_p y_{n1}(L_1)y_{m1}(L_1)(L_2+a)\cos\theta\\
&\quad+M_p\left[y_{n2}(L_2)y_{m2}(L_2)+y'_{n2}(L_2)y'_{m2}(L_2)a+y'_{n1}(L_1)y'_{m1}(L_1)(L_2+a)\right](L_2+a)\\
&\quad+\int_0^{L_2} m_{b2}\left[y_{n2}(x_2)y_{m2}(x_2)+y_{n1}(L_1)y_{m1}(L_1)\cos\theta+y'_{n1}(L_1)y'_{m1}(L_1)x_2\right]x_2\,\mathrm{d}x_2\\
&\quad+M_p\left[y_{n2}(L_2)y_{m2}(L_2)+y'_{n2}(L_2)y'_{m2}(L_2)a+y'_{n1}(L_1)y'_{m1}(L_1)(L_2+a)\right]\cos\theta\\
&\quad+(M_p+M_2)y_{n1}(L_1)y_{m1}(L_1)+\int_0^{L_1} m_{b2}\left[y_{n2}(x_2)y_{m2}(x_2)+y'_{n1}(L_1)y'_{m1}(L_1)\right]\cos\theta\,\mathrm{d}x_2\\
&\quad+\lambda_2\left[y'_{n2}(0)y'_{m2}(0)\right]+I_p\left[y'_{n1}(L_1)y'_{m1}(L_1)\right]\left[y'_{n2}(L_2)y'_{m2}(L_2)\right]\\
&\quad+M_p\left[y_{n2}(L_2)y_{m2}(L_2)+y'_{n2}(L_2)y'_{m2}(L_2)a\right.\\
&\quad\left.+y'_{n1}(L_1)y'_{m1}(L_1)(L_2+a)+y_{n1}(L_1)y_{m1}(L_1)\cos\theta\right]a\\
&\quad+M_p\left[y_{n2}(L_2)y_{m2}(L_2)+y'_{n2}(L_2)y'_{m2}(L_2)a\right.\\
&\quad\left.+y'_{n1}(L_1)y'_{m1}(L_1)(L_2+a)+y_{n1}(L_1)y_{m1}(L_1)\cos\theta\right]=0,
\end{aligned} \tag{42}$$

for any $m\neq n$. For $m=n$ the left-hand side of Eq, (42) gives a result identical to the generalised mass as obtained with the first term of Lagrange's equation:

$$\frac{\mathrm{d}}{\mathrm{d}t}\left(\frac{\partial T}{\partial\dot{q}_i(t)}\right)-\frac{\partial T}{\partial q_i(t)}+\frac{\partial V}{\partial q_i(t)}=Q_i(t), \tag{42}$$

where T denotes the system total kinetic energy, V is the potential energy and the $Q_i(t)$ are the generalised forces. Due to this fact, the off-diagonal elements of the mass matrix $\mathbf{M}$ as obtained with the first term of Eq. (42) are an indicator for the precision of the computations and a measure for the orthogonality of the eigenmodes.

For more complex systems than the examples given in the previous sections the off-diagonal elements of **M** rapidly become non-negligible with an increasing number of mode shapes. In experiments with systems more complex than the one shown in Fig. 3 the off-diagonal elements, relative to the diagonal elements, were of a magnitude of 10^{-3} for more than about five mode shapes. For systems as shown in Figs. 1 and 4 the magnitude of the off-diagonal elements relative to the diagonal elements is in the order of 10^{-6} even for more than 10 eigenmodes, and this error is assumed to be only due to rounding and limits in numerical computations. In this connection it is pointed out that these numerical limits will also occur when using any other assumed mode shape expansion. The eigenmodes as computed with the method presented here often allow for the use of only a few or even only the fundamental mode for dynamic response analyses. This is due to the well-known fact that the convergence of Eq. (41) is quicker, the more accurate the inserted mode shapes represent the real boundary conditions.

It is found that errors in numerical computations will have a more significant impact on the eigenfrequencies in relation to the impact on the eigenmodes. Due to this reason it is sometimes possible to improve results a bit by inserting computed mode shapes into Lagrange's Eq. (42) and re-compute the eigenfrequencies and eigenvectors with the system mass and stiffness matrices **M** and **K** as:

$$\left|\mathbf{K} - \omega^2 \mathbf{M}\right| = 0. \tag{43}$$

All in all, the numerical accuracy must be checked for complex beam systems, but if the characteristic determinants are not very ill-conditioned and if the results are carefully watched the proposed method to arrive at correct natural frequencies and mode shapes of any arbitrary flexible beam system proves easy and powerful.

6. Conclusions

This paper provides a method to compute the eigenfrequencies and mode shapes of any arbitrary system of interconnected Euler–Bernoulli beams subject to any arbitrary kinematic or dynamical boundary conditions.

The method is applied to some examples and its correctness is supported by means of comparison with known analytical results.

Thus this work may provide a basis of how to arrive at eigenfrequencies and mode shapes for a wide variety of beam systems and similar problems.

Acknowledgement

This seems to be a good place to say thank you to my teachers and friends Prof. Dr. Colin L. Kirk and Prof. Dr. Oskar Wallrapp.

References

[1] C.L. Kirk, S.M. Wiedemann, Natural frequencies and mode shapes of a free–free beam with large end masses, *Journal of Sound and Vibration* 254 (5) (2002) 939–949.

[2] S.M. Wiedemann, C.L. Kirk, Dynamic analysis of flexible space shuttle remote manipulator system with large payloads. *Proceedings of the Fifth International Conference on Dynamics and Control of Structures and Systems in Space*, Cambridge University, 2002.

[3] S. Timoshenko, D.H. Young, W. Weaver Jr., *Vibration Problems in Engineering*, fourth ed., Wiley, New York, 1974.

[4] R. Schwertassek, O. Wallrapp, *Dynamik flexibler Mehrkörpersysteme*, Friedrich Vieweg and Sohn Verlagsgesellschaft mbH, Braunschweig/Wiesbaden, 1999.